

# Ultra High Energy $\nu_\tau$ Detection Using Cosmic Ray Tau Neutrino Telescope

## Used in Fluorescence/Cerenkov Light Detection

Z. Cao<sup>1,2</sup>, M. A. Huang<sup>3</sup>, P. Sokolsky<sup>2</sup>, Y. Hu<sup>4</sup>

<sup>1</sup> *Institute of High Energy Physics, Beijing, 100039, China*

<sup>2</sup> *High Energy Astrophys. Inst., Univ. of Utah, Salt Lake City UT 84112 USA*

<sup>3</sup> *General Education Center, National United University, Miaoli, 360, Taiwan R.O.C.*

<sup>4</sup> *University of Science & Technology of China, Hefei, 230026, China*

### Abstract

We have investigated the possibility of  $\nu_\tau$  detection using Cosmic Ray Tau Neutrino Telescope (CRTNT) based on air shower fluorescence/Cerenkov light detector techniques. This approach requires an interaction of a  $\nu_\tau$  with material such as a mountain or the earth's crust.  $\tau$  lepton produced in the charged current interaction must escape from the earth and then decay and initiate a shower in the air. The probability for the conversion from  $\nu_\tau$  to air shower has been calculated for an energy range from 1 PeV to 10 EeV. An air shower simulation program has been developed using the simulation package Corsika. The trigger efficiency has been estimated for a CRTNT detector similar to the HiRes/Dice detector in the shadow of Mt. Wheeler in Nevada, USA. A rate of about 8 triggered events per year is expected for the AGN neutrino source model with an optimized configuration and duty cycle of the detector.



## I. INTRODUCTION

The source of cosmic rays with particle energies above  $10^{15}$  eV (1 PeV) remains unknown. A point source search could be an encouraging approach for solving this puzzle. Searches for point sources are best performed using observations of neutral particles because they can be directly traced back to the source. The universe is opaque to photons between  $10^{14}$  eV and at least  $10^{18}$  eV (1 EeV) due to interaction with the  $2.7^\circ$  K cosmological microwave background. The neutrino is another type of neutral particle that can be used to explore cosmic ray sources in this energy region. Newly discovered evidence of neutrino oscillation [1] leads to a plausible argument that the astrophysics neutrino flux will have an even flavor ratio of  $\nu_e : \nu_\mu : \nu_\tau = 1 : 1 : 1$  [2]. One obvious effect of neutrino mixing is the appearance of tau leptons. This opens a window for the cosmic ray source searches using air shower techniques since the decay products of  $\tau$  lepton, mainly hadrons and electrons, will induce a detectable shower in the air.

Neutrinos convert to electrons, muons and taus through the charged current interaction. The interaction probability is much higher in the Earth than in the atmosphere, due to the higher density of rock. However, electrons will shower quickly inside the target material. Muons travel very long distances before they decay but can only be detected by the small energy loss along the trajectory. A large detector, such as IceCube, buried inside the target material, is designed to detect those muons (track-like signals) and electrons (shower-like signals), but is inefficient for tau detection. At energies below 1 PeV, the tau decays and initiates a shower that can not be distinguished from an electron shower. At energies above 20 PeV, the tau decay distance is longer than the width of  $1 \text{ km}^3$  size detector and only one shower can be seen. At higher energies, the neutrino flux is much lower and a  $1 \text{ km}^3$  size detector is not large enough to detect such a flux.

One way to avoid constraints from the target volume is to separate of detection volume from the target volume. A fluorescence light detector such as HiRes or a Cerenkov light detector such as Dice has proven to be a successful detector with a small physical size but a huge detection volume. Leptons produced via charged current interaction must be able to escape from target volume, decay in the atmosphere and develop a shower before they reach the detector for this scheme to work. Since the Earth becomes essentially opaque to neutrinos at energy higher than 1 PeV, neutrinos come out in almost horizontal direction.



These are known as *earth-skimming neutrinos* [3, 4]. The conversion efficiency from a tau neutrino to a tau is approximately  $R_d\rho/\Lambda_I$ , where  $\rho$  is target density.  $R_d$  is range of the tau in the target and  $\Lambda_I$  is interaction length in the target [5]. At energies above 1 PeV, tau leptons have a range such that the conversion probability in the Earth is higher than that in the atmosphere [6]. The conversion efficiency becomes much higher at higher energy because  $R_d$  increases less than linearly with energy but  $\Lambda_I$  grows proportional to  $E^{-2.36}$  [7]. This unique mechanism of detecting  $\tau$ -neutrino provides an acceptance that is much larger than 1 km<sup>3</sup> underwater/under-ice detector arrays, especially at energy higher than 10 PeV. Detecting the tau lepton from earth-skimming neutrinos becomes an excellent way to study ultra high energy neutrino astronomy and to provide a possible proof of neutrino flavor oscillation.

The rest of paper is organized as following. In Section II, the conversion from tau neutrino to air shower and possible shower detection are discussed. The CRTNT detector is proposed at a potential site. A simulation of  $\nu_\tau$  to  $\tau$  conversion, shower development and shower detection is described in Section III in detail. The event rate and its optimization are presented in Section IV. Final conclusions are summarized in the last section.

## II. FEASIBILITY STUDY

We first try to evaluate the detection of tau neutrinos skimming through mountains, then discuss the detection techniques and a potential site for the proposed CRTNT project.

### A. $\nu_\tau$ to air shower conversion

Two coordinate systems are used in this study. A three dimensional local coordinate system describes the detector position and local topological information. The other is an one-dimensional coordinate system along the neutrino trajectory used for describing the mountain-passing/Earth-skimming process. The trajectory is described by the elevation angle  $\epsilon$ , the azimuth angle  $\phi$ , and the location of the escape point from the mountain/earth surface  $(x_e, y_e, z_e)$  in the 3-D local coordinate system. In the 1-D coordinate system,  $\nu_\tau$ 's travel from negative infinity and enter the mountain at  $r = -T$ , where T is the thickness of the mountain or the earth's crust. The density distribution  $\rho(r)$ , and the total path length  $T$

are different depending on the geometry of the trajectory. The incident  $\nu_\tau$  interacts between  $-T$  and 0, the  $\tau$  then decays and initiates a shower at  $r$ . The probability of such a conversion from  $\nu_\tau$  to a shower is a convolution of interaction probability of  $\nu_\tau$  before distance  $r$  and the probability of decay to a shower at  $r$ . It simplified to

$$p_c(r; T)dr = \begin{cases} \frac{1}{1-e^{-T\rho/\Lambda}} \frac{dr}{R_d-\Lambda_I/\rho} \left[ e^{-\frac{r+T}{R_d}} - e^{-\frac{r+T}{\Lambda_I/\rho}} \right] & (-T < r < 0) \\ \frac{1}{1-e^{-T\rho/\Lambda}} \frac{dr}{R_d-\Lambda_I/\rho} \left[ e^{-\frac{r}{R_d}} - e^{-\frac{r}{\Lambda_I/\rho}} \right] e^{-\frac{r}{R_d}} & (r \geq 0) \end{cases} \quad (1)$$

where  $p_c(r; T)$  is the conversion probability density (CPD) for a given trajectory  $T = T(\epsilon, \phi, x_e, y_e)$ ,  $\lambda_I$  is the  $\nu_\tau$  interaction length in  $g/cm^2$  and  $R_d$  is the average range of  $\tau$ -lepton in km, i.e.  $R_d = f\gamma c\tau$  where  $\gamma$  is the Lorentz boost factor,  $\tau$  is the lifetime of the  $\tau$ -lepton and  $f$  is a fraction accounting energy loss [8].  $f$  decreases from 0.8 at  $E_\tau = 100$  PeV to 0.2  $E_\tau = 1$  EeV [5]. FIG. 1 shows two cases of the CPD's as functions of  $r$  corresponding to down-going ( $\epsilon > 0$ , through a mountain about 21 km thick) and up-going earth-skimming ( $\epsilon < 0$ , through the earth's crust about 1300 km thick) trajectories.

As shown in FIG. 1, for energies lower than 10 PeV, the CPD is flat because of the long interaction length of the  $\nu_\tau$  and the short decay length of the  $\tau$  lepton. Only primary  $\nu_\tau$ 's that interact close to the surface can produce an observable  $\tau$ . For  $E_\nu$  above 10 PeV, the CPD peaks around 10-20 km in thickness of rock. The energy loss in the target material reduces both the survival rate and the energy of  $\tau$ 's above  $10^{17}$  eV. These results are consistent with other recent calculations [4, 5].

### B. Detection of earth skimming $\nu_\tau$

The  $\tau$  lepton flux induced by an earth-skimming neutrino flux will be orders of magnitudes lower than the cosmic ray flux in the observational window, a range from 1 PeV to 10 EeV [9]. A successful detection would require a detector having a large acceptance, on the order of several  $km^2$  sr to over  $100 km^2$  sr. Because most of earth-skimming neutrinos are concentrated near the horizon, the detector should have a great sensitivity to horizontal showers. Ground detector arrays have small trigger efficiency for both upward and downward going showers in the vicinity of horizontal direction and hence can not be very efficient for detecting  $\nu_\tau$ . Detection through optical signals would seem to be more efficient. A combination of fluorescence light and Cerenkov light detector in a shadow of a steep cliff could achieve this goal.

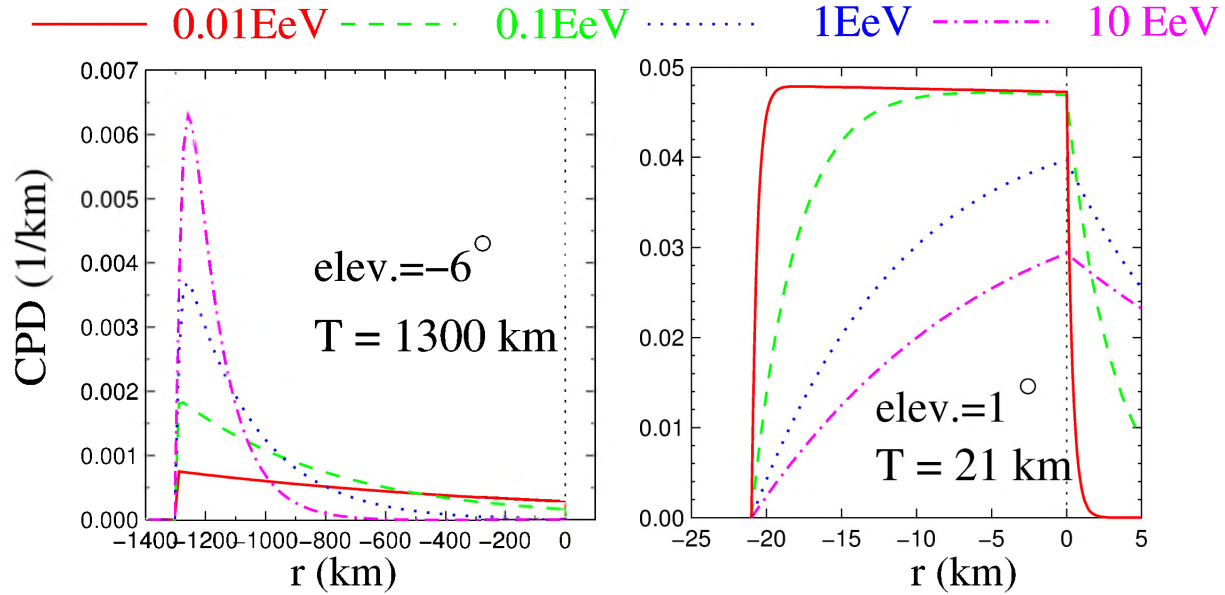


FIG. 1:  $\nu_\tau$  to shower conversion probability density (CPD) as a function of distance along trajectory.

A fluorescence light detector, such as the HiRes prototype experiment [10], has a large FOV and acceptance. The difficulty is that it has to be operated at a high threshold corresponding to above 0.3 EeV, because of noise from sky background light. Cerenkov radiation provides many more photons along the shower axis. It can be useful for lowering the detection threshold. The Dice Experiment [11] successfully measured the energy spectrum and composition of cosmic rays between 0.1 PeV and 10 PeV using the same detector but triggered by Cerenkov light. To maintain a good energy resolution, a typical Cerenkov telescope has to be operated within a small FOV of about a few degrees with respect to the air shower since the Cerenkov light intensity is a rapidly decreasing function of the viewing angle. On the other hand, a fluorescence light detector has to be operated with large viewing angle to the shower axis to avoid significant Cerenkov light contamination that can cause poor shower energy resolution. In order to achieve satisfactory statistics for the neutrino flux measurement, we have to lower the threshold while maintain a large aperture.

Several points need to be stressed. First of all, the shower energy resolution is not crucial for neutrino searches, hence the Cerenkov light can be tolerated and can be useful for triggering the detector. Secondly, sky noise can be suppressed by placing the detector in the shadow of a mountain. A steep mountain in front of the detector is shown to be a good



target for neutrino conversion in the above discussion. It also serves as a screen to block sky noise. Because of the low light background, the detector can be operated with a lower threshold as a fluorescence light detector. More importantly, the background from cosmic rays at the same or lower energies is much reduced. This makes the  $\nu_\tau$  events distinguishable from cosmic ray events. Finally, to enlarge the FOV of the detector, the telescopes can be configured to surround the mountain and minimize overlaps between telescopes.

In order to obtain sufficient fluorescence and Cerenkov light, we have to have a sufficient space for air shower development. A steep mountain side provides a large elevation coverage for the detector and a large open space between the mountain surface and the detector. An ideal site for observations would be by a steep mountain and in a dry and clear atmospheric environment essential for fluorescence/Cerenkov light techniques.

In this paper, we consider placing the CRTNT detector in proximity to Mt. Wheeler Peak(3984 m a.s.l.) near the Nevada-Utah border, USA. The mountain lies in a north-south direction and is about 40 km long. The west side is very steep. Further west, there is a flat valley about 30 km wide at about 1500 m a.s.l. For a detector located about 12 km away from the peak horizontally, the shadow of the mountain is about  $11.7^\circ$  in elevation. It almost completely blocks the FOV of the telescopes of the CRTNT detectors proposed below. Within the shadow, the sky noise background should be less than that from the open sky. At Dugway, Utah, about 120 km north of the Wheeler Peak, the light background was measured to be  $40 \text{ photon}/\mu\text{sec}/\text{m}^2$ . In this paper, the light background for all the telescopes in the shadow is assumed to be the same as at Dugway. This is the upper limit to the sky noise. An on-site measurement for the actual background light will be done using a prototype detector.

### C. The CRTNT fluorescence/Cerenkov light detector

The proposed CRTNT project uses fluorescence/Cerenkov light telescopes analogous to the detectors of the HiRes and the Dice experiments[19]. The telescopes are distributed in three groups located at three sites separated by eight km in the valley facing the west side of Mt. Wheeler Peak. At each site, four telescopes observe an area of the mountain with  $64^\circ$  in azimuth and  $14^\circ$  in elevation. This area is about 14 km long in the north-south direction. The total field of view covers about  $60^\circ \times 14^\circ$  and  $70 \text{ km}^2$  with small overlaps between the

telescopes on the three sites.

A 5.0 m<sup>2</sup> light collecting mirror with an reflectivity of 82% is used for each telescope. The focal plane camera is made of 16×16 pixels. Each pixel is a 44 mm hexagonal photomultiplier tube that has about a 1° × 1° field of view. Each tube is read out by 50 MHz flash ADC electronics system to measure the waveform of the shower signals

A pulse area finding algorithm is developed for providing an individual channel trigger using field programmable gate array (FPGA). The first level trigger is set by requiring the signal-noise ratio to be greater than 4 $\sigma$ , where the  $\sigma$  is the standard deviation of the total photo-electron noise during the signal pulse. The noise level is different for each pulse because the pulse duration varies depending on the distance to the light source. The second level trigger requires at least five channels triggered within a 5×5 running box over a single telescope camera of 16×16 pixels. The trigger condition for an event is that at least one telescope is triggered. All triggers are formed by FPGA chips. Event data from all channels are scanned with a threshold lower than the trigger threshold from the FPGA buffers into a local Linux box.

A Monte Carlo simulation program for the detector is developed as described in the next section. Thousands of showers initiated by the products of  $\tau$ -decays and normal cosmic rays are generated. Two simulated event examples are shown in FIG.2. In FIG.2 a), a  $\tau$  neutrino induced air shower starts in the shadow of the mountain where a normal cosmic ray event is not expected. By contrast, a normal cosmic ray event is shown in FIG.2 b). FIG.3 shows the detector configuration and shower initial point locations.

### III. MONTE CARLO SIMULATION

In the simulation, the incident  $\nu_\tau$  is coming from an interval of elevation angles between  $-11^\circ$  and  $17^\circ$ , where the negative direction means a upward-going neutrino. The azimuth range is from  $90^\circ$  to  $270^\circ$ , with all directions from the back of the mountain (the x-axis is pointing to the East). The flux of neutrino is assumed to be isotropic and uniform in the field of view of the detector. Every incident  $\nu_\tau$  is tested to see if it interacts inside the rock. The energy and momentum of the produced  $\tau$  are traced until its decay in the case that the neutrino interacted. The energy loss and the range of  $\tau$  lepton are calculated according to the result of Ref. [8]. If the  $\tau$  decays outside the rock, there is about an 80% probability that

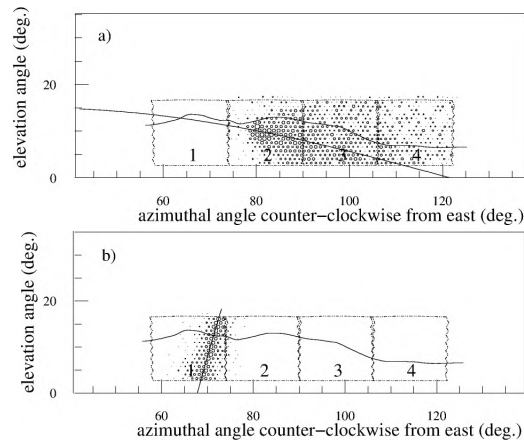


FIG. 2: Simulated air showers seen by the CRTNT detector. a) A  $\tau$  neutrino induced air shower starting and developing completely in the shadow of the mountain. The line along the shower direction represents a plane which contains the detector and the shower axis. The dashed lines show the boundary of the field of view of each telescope. The thick solid curve represents the profile of the Mt. Wheeler Peak. Circles represent triggered tubes and the size of each circle is proportional to the logarithm of the number of photons seen by the tube. b) A normal cosmic ray air shower event coming down and hitting on the slope of the mountain.

an electron or multiple hadrons, mainly pions or kaons, are produced in the decay. Those particles will initiate electromagnetic or hadronic showers from the decay point. The shower type and energy are determined by a standard  $\tau$  decay routine and passed to an air shower generator. However, if the  $\tau$  flies too far from the mountain surface before its decay, showers could be initiated behind the detector and would not be detected. In the simulation,  $\tau$ 's that decay anywhere further than 7 km from the escape point on the mountain surface are ignored.

On the other hand, if the  $\tau$  decays inside the rock, a regeneration procedure will be started in the simulation. This procedure repeats the previous process using the decay-product  $\nu_\tau$  whose energy is determined by the same  $\tau$ -decay routine mentioned before. Since the energy reduction is rather large in the  $\nu_\tau$  to electron/hadron conversion, there is no need to repeat this regeneration procedure in further decays because the shower energy is lower than the threshold of the detector. The regenerated  $\tau$ 's which decay inside the rock again are ignored.



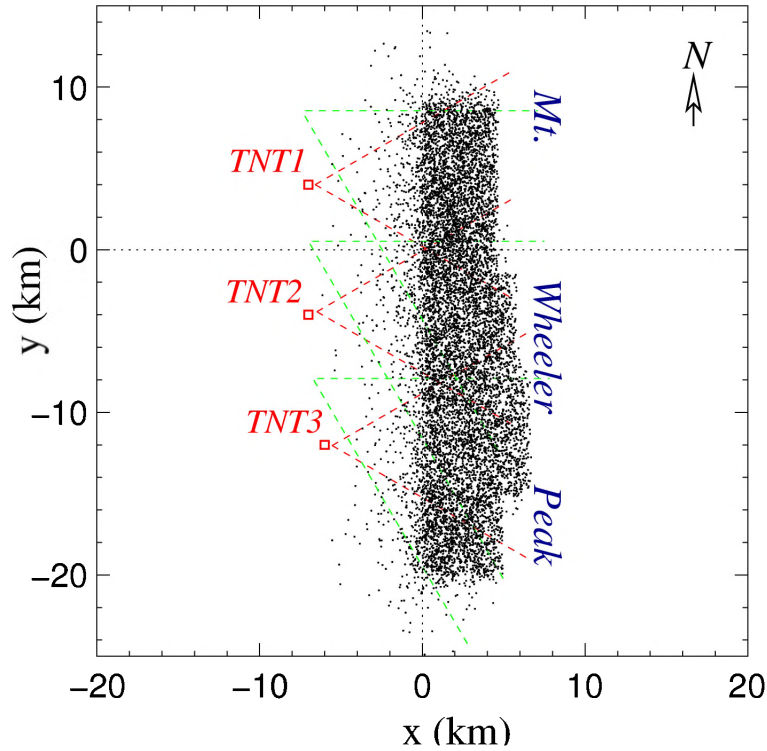


FIG. 3: Locations of initiating points of showers induced by  $\tau$  neutrinos through MT. Wheeler Peak near Utah/Nevada border. The squares represent CRTNT telescopes. The solid lines attached to the detectors indicate the FOV of the telescopes. The dashed lines show a further optimization idea for catching  $\nu_\tau$ 's from the center of our galaxy. See text in Conclusion section for details.

#### A. From tau neutrino to tau lepton

The  $\nu_\tau$  to shower conversion efficiency is defined as the ratio between the total number of successfully converted events and the number of incident  $\nu_\tau$ 's. The simulation yields the conversion efficiency of  $1.99 \times 10^{-4}$  and  $2.21 \times 10^{-2}$  for the AGN[12] and GZK[16] neutrino source models, respectively. A distribution of locations where showers start developing is shown in FIG. 3. The detectors and their fields of view are shown in the same figure. The distributions of trigger efficiency as a function of energy are shown in FIG. 6 and FIG. 5. The conversion probability is different for different models mainly because the GZK neutrino energy spectrum is much harder than the AGN's, therefore they have a different pile-up effect associated with  $\tau$  energy-loss.

Because of the rather strong energy loss of the  $\tau$  through ionization and radiation, the energy of re-converted shower via  $\nu$ -regeneration is significantly lower. The contribution



from the  $\nu_\tau$ -regeneration to the final detectable shower event rate is not significant. The regenerated  $\nu_\tau$ -shower conversion efficiency is less than 0.6% and 2.0% of the total conversion efficiency for AGN and GZK neutrinos, respectively.

### B. Air Shower Simulation

Corsika 6.0 [17] is used to generate air showers in the space between shower initiating point outside the mountain and the CRTNT telescopes. Because the detector is located about 12 km away from the mountain peak horizontally, the typical distance available for shower development is about 10 km in the air. Since all showers are initiated in an almost horizontal direction, the air density along the path of the shower development is nearly constant. Thus a uniform air density is assumed for the air shower development. A simulated shower library is established by generating 200 hadronic and 200 electromagnetic showers at three values of  $1\times$ ,  $2\times$  and  $5\times$  of energies in each order of magnitude between 10 PeV and 1 EeV. The shower longitudinal profiles, i.e. number of charged shower particles along the shower axis, are stored in the library at every  $5 \text{ g/cm}^2$ .

Once a  $\tau$  decays outside the mountain surface, it starts an air shower except if the decay product is a  $\mu$ . The decay point is taken as depth zero  $\text{g/cm}^2$  for the shower development. A shower profile is randomly selected from the library in the group of showers at the closest energy. The number of charged particles of this picked shower are scaled up or down to represent the shower to be simulated. The amount of scaling is determined by the difference between the given shower energy and the energy of the selected shower. Some shower examples are shown in FIG.4. Note that the longitudinal development behavior is quite different from that of showers that develop from the top of the atmosphere to the ground where the density of the air increases nearly exponentially. Moreover, the hadronic showers develop noticeably faster than electromagnetic showers.

### C. Photon production and light propagation

Charged shower particles excite the nitrogen molecules as they pass through the atmosphere. The deexcitation of the molecules generates ultra-violet fluorescence light. The number of fluorescence photons is proportional to the shower size and these photons are

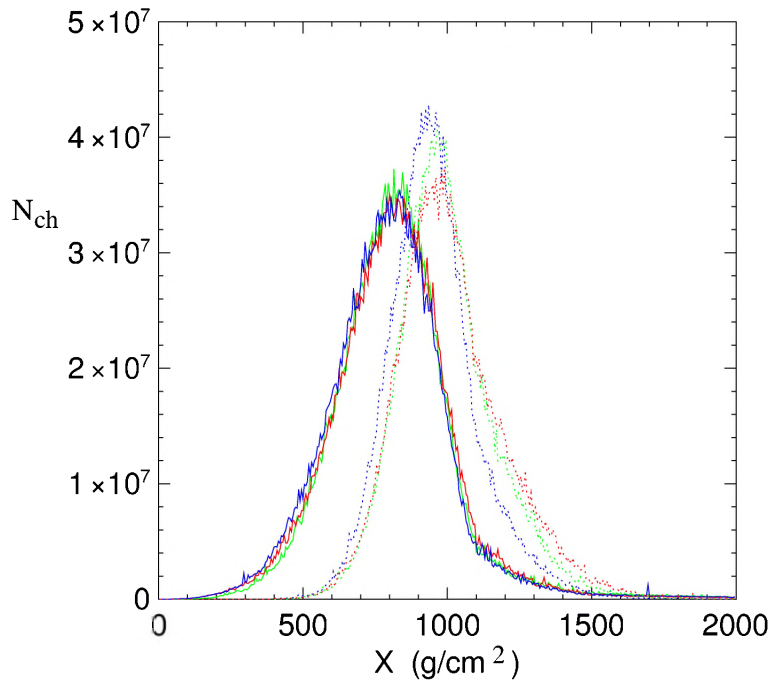


FIG. 4: Showers generated by Corsika at energy  $5 \times 10^{16}$  eV. Solid lines are hadronic showers. Dotted lines are electron showers.

emitted isotropically. The shower simulation carried out in this paper assumes a fluorescence light spectrum according to a recent summary of world wide measurements[18], including the dependence of the yield to the atmospheric pressure and temperature.

Since energies of charged shower particles are higher than the critical energy, the shower particles generate Cerenkov photons at every stage of the shower development. The accumulated Cerenkov light concentrates in a small forward cone, therefore the intensity of the light is much stronger than the fluorescence light along the shower direction. Even for low energy showers at 500 TeV, the strong forward Cerenkov light beam can be detected if the shower comes directly toward the detector. For shower coming from other directions, a significant part of the Cerenkov light is scattered out via Rayleigh and Mie scattering during the whole shower development history. The fraction of this light scattered in the direction of the detector can also make a noticeable contribution to detector triggering.

The procedure of Cerenkov light generation and scattering is fully simulated. Detailed description about the calculation can be found in Ref. [19] and references therein.

Shower charged particles and therefore fluorescence light photons, spread out laterally following the NKG distribution function. The Moliere radius parameter of the NKG function



is about 95 m at about 1500 m a.s.l. Photons originating from Cerenkov radiation have an exponential lateral distribution from the axis of the shower. Therefore, photons coming from a shower are spread over a range of directions around the shower location in the sky due to its longitudinal motion and lateral extension. A ray tracing procedure is carried out to follow each photon to the photo-cathode of PMT's once the photon source is located in the sky. All detector responses are considered in the ray tracing procedure, including mirror reflectivity, UV filter transmission, quantum efficiency of photo-cathode, location-sensitive response function of the photo-cathode and optical effects associated with the off-axial and defocus effects. The technical parameters of the detector are set to be the same as the existing HiRes detector. More details on the detector specifications can be found elsewhere[19].

Sky noise photons are randomly added in this ray tracing procedure both in time and arrival directions.

The uncertainty associated with the varying weather conditions is negligible for the Rayleigh scattering. The Mie scattering due to the aerosols is more dependent of the weather condition that drives the aerosol distribution. However, for a detector that has an aperture within 6 km, the aerosol scattering contribution to the light extinction is close to minimum. The uncertainty in the triggering efficiency due to weather conditions is thus small. In the simulation, an average model [20] of aerosol scattering for standard desert in west US is employed.

#### IV. PREDICTED EVENT RATE

For the CRTNT detector, we calculate the event rate using the  $\nu_\tau$  to air shower conversion algorithm and the shower/detector simulation described above. Since the primary neutrino energy spectra are different in different production models, induced air showers from different sources have slightly different detection efficiency. In order to illustrate the difference, two extreme cases are simulated in this paper. For a model dominated by low energy neutrinos (still above the threshold of the CRTNT detector), we use the AGN neutrino source model [12]. For a model with many more higher energy neutrinos, we use the GZK neutrino source model [16]. We generate  $10^9$  and  $10^7$  trials for AGN and GZK models, respectively.

Due to the stronger energy loss of the higher energy  $\tau$  leptons, the observed GZK neutrino

spectrum is severely distorted. The high energy neutrinos pile up at low energies once they are converted into lower energy showers. On the other hand, the shower triggering simulation shows that the trigger efficiency is slightly higher for higher energy showers. The competition between those two effects yields a relatively flat event rate distribution between 10 PeV and 2 EeV. The distribution is shown in FIG.5. The overall detection efficiency is  $2.4 \times 10^{-3}$ . According to the flux suggested by authors of [16] and a typical 10% duty cycle of the fluorescence/Cerenkov light detector, the event rate is about  $0.23 \pm 0.01$  per year.

The predicted AGN neutrino flux in Ref. [21] is ruled out by the AMANDA experiment [22]. In this paper, we use an updated prediction of the AGN neutrino spectrum [12]. The source spectrum changes from  $\sim E^{-1}$  to  $\sim E^{-3}$  near 10 PeV. The neutrino flux is cut off around 0.6 EeV. In this case, the energy loss of the  $\tau$  lepton inside the mountain is no longer significant. The converted shower spectrum has a similar shape to the incident neutrino spectrum at high energies. The conversion efficiency drops rapidly with energy in the low energy region. This softens the event rate as a function of energy below 10 PeV.

The average trigger efficiency of showers induced by the products of  $\tau$ -decays is 11.0%. The overall detection efficiency of AGN neutrinos is  $2.19 \times 10^{-5}$ . The spectra of  $\nu_\tau$  are shown in FIG. 6. According to the flux predicted by authors of [12], the event rate is  $5.04 \pm 0.05$  per year, where a 10% duty cycle is assumed for the detector.

### A. Optimization

Using the simulation tool, we have tried to optimize the configuration of the detector to maximize the event rate. We find that the distances between the telescopes and the mountain are important parameters. Without losing much of the shadow size, the detection efficiency is higher if the telescopes are placed further from the mountain up to the distances of about 12 km. For the site near Mt. Wheeler Peak, the altitude of the detectors are about 1500 m a.s.l. at 12 km from the mountain. This yields about a  $11.7^\circ$  shadow on the detector. A single layer detector configuration shown in FIG.2 maximizes the trigger efficiency of the neutrino detection. Using an array configuration of three single layer detectors separated by 8 km (see FIG.3) maximizes the usage of the mountain body as a  $\nu_\tau$  to shower converter.

Since the detector has a limited field of view toward the east, more than 3/4 of field of view of telescope is covered by the mountain shadow. The moon will not be in the field

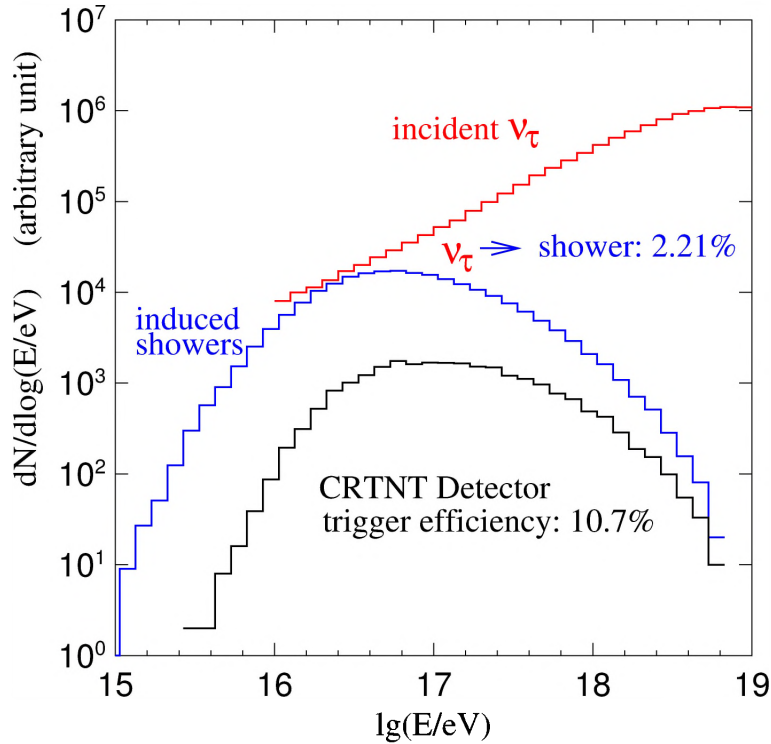


FIG. 5: GZK  $\nu_\tau$  to air-shower conversion and triggering rate. The incident  $\nu_\tau$  energy spectrum, converted shower energy distribution are plotted. The triggered air-shower event distribution is calculated based on a detector described in Sec. IIC and an air-shower development algorithm described in Sec. IIIB.

of view most of night time. The level of scattered moon light toward the detector will be sufficiently low when the moon moves behind of the telescopes. The detector should be able to be operated under such condition. Conservatively, the useful observation time can be then increased by 50%. A rate of about 8 events per year could then be expected for the AGN model case. More accurate estimate requires an on-site measurement for the light background with the moon up.

In this paper,  $\nu_e$ 's and  $\nu_\mu$ 's are not taken into account. From the point of view of  $\tau$  neutrino search, showers induced by these neutrinos are background. However, for the purpose of particle astronomy, these neutrinos carry the same information about the source as the  $\nu_\tau$  does. Since the  $\mu$  generated in  $\nu_\mu + A$  interaction hardly interacts and does not initiates a shower in the air, there is nearly no chance for it to trigger the detector. However, both  $\nu_e$  and  $\nu_\mu$  transfer 20% to 30% of energy to the target in the deep inelastic scattering (DIS) processes. The fragments of the target particles can induce detectable showers in

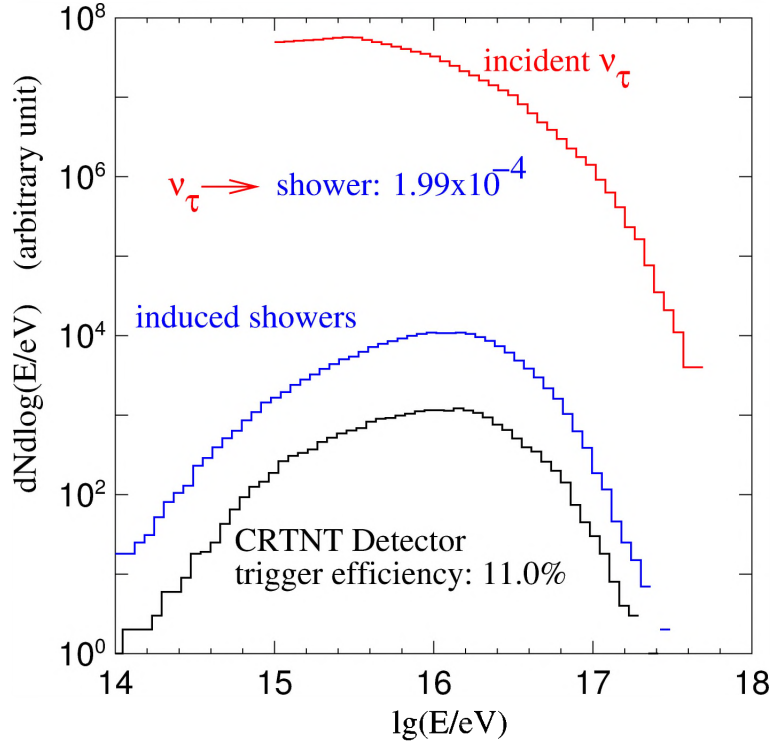


FIG. 6: AGN  $\nu_\tau$  to air-shower conversion and triggering rate. The incident  $\nu_\tau$  energy spectrum and converted shower energy distribution are plotted. The triggered air-shower event distribution is calculated according to a detector described in Sec. II C and an air-shower development algorithm described in Sec. III B.

the air if the neutrinos interact in a very thin layer of rock right beneath the surface. The contribution of the DIS processes could be enhanced because the neutral current processes also contribute to the detectable air shower generation.  $\sigma_{CC} + \sigma_{NC}$  is the effective DIS cross section, in which the neutral current cross section  $\sigma_{NC}$  is about 44% of the charged current cross section  $\sigma_{CC}$  at  $10^{15}$  eV and 31% at  $10^{20}$  eV [7]. The interaction length for these processes is still very long, e.g.  $6.6 \times 10^8$  g/cm<sup>2</sup> for  $10^{16}$  eV and  $2.2 \times 10^7$  g/cm<sup>2</sup> for  $10^{20}$  eV. Since the total thickness of the mountain is about 20 km, i.e.  $5.2 \times 10^6$  g/cm<sup>2</sup>, we can assume the free paths of neutrinos to be a uniform distribution. Assuming that only DIS's which happened within a layer of one to two radiation length behind the mountain surface are able to generate detectable showers, the DIS event conversion efficiency is approximately  $5 \times 10^{-6}$ . Comparing the  $\nu_\tau$ -shower conversion efficiency approximately  $3 \times 10^{-4}$  at  $10^{16}$  eV, the ratio of DIS events versus  $\nu_\tau$  events is only about 1.7%.

For higher energies, the mean free path of the neutrino is shorter but only by one order of



magnitude over three decades of energies. Thus the flat free path distribution is still a good approximation. The  $\nu_\tau$ -shower conversion efficiency increases with energy rather rapidly. The ratio between number of DIS events and number of  $\nu_\tau$  events reduces to 0.04% at  $10^{19}$  eV.

## V. CONCLUSION

The technique of using a mountain to convert  $10^{16} \sim 10^{19}$  eV neutrinos to air showers and using fluorescence/Cerenkov light to detect the showers can be optimized by setting the detector near a  $\sim 20$  km thick mountain body. Mt. Wheeler near the Nevada/Utah border is a good example of maximizing the conversion in this energy range. The energy reduction in the conversion process is so severe for high energy  $\tau$ 's that showers pile up below  $10^{17}$  eV in the shower energy spectrum. The regeneration of  $\nu_\tau$  is found to have an insignificant effect on the conversion of  $\nu_\tau$  to air shower, a contribution of less than two percent. Cerenkov light may dominate over fluorescence light and become the main light source to trigger the CRTNT detectors. An air shower development algorithm has been developed using Corsika in a uniform atmosphere for estimating trigger efficiency. Fluorescence/Cerenkov light production and propagation are fully simulated. Detector response is also fully simulated. The detector configuration is optimized using this simulation tool. The CRTNT detector simulation indicates that a rate of about 8 events per year for an optimized detector with 15% duty cycle is expected for the AGN source model[12].

With such a sensitivity, the CRTNT detector can be used for searching for nearby cosmic ray sources, e.g. our galactic center (GC). Since gamma rays are blocked by dust near the GC and cosmic rays are bent away from the GC due to the strong magnetic field around the GC, the neutrino is a unique particle can be used for exploring the GC region. At the site near Mt. Wheeler Peak, the GC rises above the horizon in summer night and reaches its highest elevation about  $20^\circ$ . The GC would be well covered by the CRTNT detector if the detectors face south. Therefore, to make a balance between the use of the mountain as a converter and the duration in which the GC being seen, we turn all telescopes about  $30^\circ$  to the south. The field of view of the reconfigured CRTNT detector is shown in FIG.3 by the dashed lines. The neutrino event trigger efficiency would not be changed much, however, about 1000 hour exposure could be expected during a run of three years.





## VI. ACKNOWLEDGMENTS

MAH and ZC are grateful to G.L. Lin and J.J. Tseng for theoretical support. Many thanks from ZC to R.W. Springer for very fruitful discussions. This work (ZC) is partially supported by Innovation fund (U-526) of IHEP, China and Hundred Talents & Outstanding Young Scientists Abroad Program (U-610) of IHEP, China. ZC and PS are partially supported by US NSF grants PHY 9974537 and PHY 9904048, while MAH is supported by Taiwan NSC grant 92-2119-M-239-001.

- 
- [1] Y. Fukuda *et al.* (Super-Kamiokande Coll.), Phys. Rev. Lett., **81**, 1562, (1998); *ibid.* **82**, 1810, (1999); **85**, 3999, (2000).
  - [2] H. Athar, M. Jezabek, O. Yasuda, Phys.Rev. D62, 103007, (2000); J. F. Beacom, P. Crotty and E. W. Kolb, Phys. Rev. **D66**, 021302(R), (2002).
  - [3] J. L. Feng *et al.*, Phys. Rev. Lett. **88**, 161102, (2002) and references therein.
  - [4] D. Fargion, Astrophys. J. **570**, 909,(2002).
  - [5] G. W. S. Hou and M. A. Huang, Proc. of the First NCTS Workshop on Astroparticle Physics, Kenting, Taiwan. Ed. by H. Athar, G.L. Lin, K.N. Ng, P.105, World Sci., Singapore, (2002).; astro-ph/0204145, (2002).
  - [6] M. A. Huang, J. J. Tseng, and G. L. Lin, Proc. of the 28th ICRC, Tsukuba, Japan, 1427, (2003)
  - [7] R. Gandhi *et al.*, Phys. Rev. **D58**, 093009, (1999).
  - [8] S. I. Dutta *et al.*, Phys. Rev. **D63**, 094020, (2001).
  - [9] J. J. Tseng *et al.*, Phys. Rev. **D68**, 063003, (2003).
  - [10] T. Abu-Zayyad *et al.*, Astrophys. J. **557**, 686, (2001).
  - [11] S. P. Swordy and D. B. Kieda, Astropart. Phys. **13**, 137, (2000).
  - [12] D. Semikoz and G. Sigl, JCAP 0404,3 (2004).
  - [13] A. Waxman and J. Bahcall, Phy. Rev. Lett. **78**, 2292, (1997).
  - [14] G. Sigl *et al.*, Phy. Rev. **D59**, 043504, (1998).
  - [15] Yoshida, Sigl, and Lee, Phy. Rev. Lett. **81**, 5055, (1998).
  - [16] F. W. Stecker *et al.*, Phy. Rev. Lett. **66**, 2697, (1991).



- [17] D.Heck *et al.*, *preprint of Institut fur Kernphys., Univ. of Karlsruhe*, FZKA-6019, Feb., 1998 (Kernforschungszentrum, Karlsruhe, 1998).
- [18] M.Nagano *et al.*, "NEW MEASUREMENT ON PHOTON YIELDS FROM AIR AND THE APPLICATION TO THE ENERGY ESTIMATION OF PRIMARY COSMIC RAYS", astro-ph/0406474 (2004).
- [19] T.Abu-Zayyad *et al.*, *Astrophys. J.* **557**, 686, (2001).
- [20] R.U.Abbasi *et al.*, "Techniques for Measuring Atmospheric Aerosols for Air Fluorescence Experiments", submitted to *Astropart. Phys.*, (2004)
- [21] B. W. Stecker and M. H. Salamon, *Space Sci. Rev.* **75**, 341, (1996).
- [22] G. C. Hill, for the AMANDA coll., *Proceedings of the XXXVIth Recontres de Moriond, Electroweak Interactions and Unified Theories*, March 2001 (astro-ph/0106064).